PNAS RESEARCH ARTICLE | EARTH, ATMOSPHERIC, AND PLANETARY SCIENCES
PLANT BIOLOGY

Isotopic clumping in wood as a proxy for photorespiration in trees

Max K. Lloyd[a,b,1], Rebekah A. Stein[a,c], Daniel E. Ibarra[a,d], Richard S. Barclay[e], Scott L. Wing[e], David W. Stahle[f], Todd E. Dawson[g], and Daniel A. Stolper[a]

Edited by Donald Ort, University of Illinois at Urbana Champaign, Urbana, IL; received April 24, 2023; accepted September 22, 2023

Photorespiration can limit gross primary productivity in terrestrial plants. The rate of photorespiration relative to carbon fixation increases with temperature and decreases with atmospheric [CO_2]. However, the extent to which this rate varies in the environment is unclear. Here, we introduce a proxy for relative photorespiration rate based on the clumped isotopic composition of methoxyl groups (*R*–O–CH_3) in wood. Most methoxyl C–H bonds are formed either during photorespiration or the Calvin cycle and thus their isotopic composition may be sensitive to the mixing ratio of these pathways. In water-replete growing conditions, we find that the abundance of the clumped isotopologue $^{13}CH_2D$ correlates with temperature (18–28 °C) and atmospheric [CO_2] (280–1000 ppm), consistent with a common dependence on relative photorespiration rate. When applied to a global dataset of wood, we observe global trends of isotopic clumping with climate and water availability. Clumped isotopic compositions are similar across environments with temperatures below ~18 °C. Above ~18 °C, clumped isotopic compositions in water-limited and water-replete trees increasingly diverge. We propose that trees from hotter climates photorespire substantially more than trees from cooler climates. How increased photorespiration is managed depends on water availability: water-replete trees export more photorespiratory metabolites to lignin whereas water-limited trees either export fewer overall or direct more to other sinks that mitigate water stress. These disparate trends indicate contrasting responses of photorespiration rate (and thus gross primary productivity) to a future high-[CO_2] world. This work enables reconstructing photorespiration rates in the geologic past using fossil wood.

photorespiration | clumped isotopes | methoxyl groups | lignin | climate change

Plants and climate are inextricably linked. For example, plants affect Earth's climate by removing CO_2 from the atmosphere [e.g., (1–3)], by modifying silicate weathering rates [e.g., (4, 5)] and by altering local hydrologic cycles [e.g., (6, 7)]. Earth's climate in turn affects plants via the dependence of plant carbon assimilation rates on variables including temperature, the concentration of CO_2 and O_2 in the atmosphere ([CO_2], [O_2]), and water availability in a given environment [e.g., (8–10)]. As such, the response of plants to changes in climate is critical to constraining terrestrial carbon cycling in past, present, and future climate states on both relatively short (decadal) and geologic (million year) timescales (11–14).

One key variable in the global carbon cycle is gross primary productivity (GPP), which quantifies how much CO_2 plants fix prior to respiration and sets how much CO_2 the terrestrial biosphere removes from the atmosphere as a function of time (15). Terrestrial GPP is influenced by variables such as temperature and the availability of light, water, and nutrients in a given environment. One major constraint on GPP is photorespiration, which occurs concurrently with photosynthesis in C3 plants when the enzyme Rubisco (ribulose-1,5-biphosphate carboxylase oxygenase) oxygenates its substrate with O_2 instead of carboxylating it with CO_2. This oxygenation creates toxic intermediates that are metabolically recycled by the photorespiration pathway, during which some previously assimilated carbon is released as CO_2 (16–19). If photorespiration rates increase relative to carboxylation, then less CO_2 is fixed overall, decreasing GPP. The relative rate of oxygenation to carboxylation for a given Rubisco (hereafter the relative photorespiration rate) increases with increasing temperature and decreases as the ratio of [CO_2] to [O_2] increases at the site of the reaction (8, 10, 19–22). Relative photorespiration rates are thought to be significant in modern ecosystems—for example, models estimate that at 25 °C in an atmosphere with 350 ppm [CO_2], on average 25% of CO_2 initially assimilated by modern C3 plants at 25 °C is rereleased through photorespiration (19, 20). However, the extent to which an individual plant in a given ecosystem adheres to or departs from this average is hard to predict and depends on many physiological and environmental factors that may or may not be known.

Significance

Photorespiration occurs when, during photosynthesis, plants consume O_2 and release CO_2 instead of the reverse. How photorespiration varies in the environment today is uncertain but important for validating how climate will change in the future and has changed in the distant past. We develop and apply a proxy for photorespiration rate based on the isotopic composition of a specific functional group (methoxyl) in wood. This proxy varies systematically with growing temperature and water availability of trees globally, which suggests that plants in different ecosystems photorespire different amounts and have different physiologic and metabolic responses to climate. Whether plants photorespire more or less in the future and geologic past depends on how local temperature and water availability scale with atmospheric CO_2.

Author contributions: M.K.L. and D.A.S. designed research; M.K.L. and R.A.S. performed research; M.K.L., D.E.I., R.S.B., S.L.W., D.W.S., and T.E.D. contributed new reagents/analytic tools; M.K.L., R.A.S., T.E.D., and D.A.S. analyzed data; and M.K.L., R.A.S., D.E.I., R.S.B., S.L.W., D.W.S., T.E.D., and D.A.S. wrote the paper.

The authors declare no competing interest.

This article is a PNAS Direct Submission.

[1]To whom correspondence may be addressed. Email: mlloyd@psu.edu.

This article contains supporting information online at https://www.pnas.org/lookup/suppl/doi:10.1073/pnas.2306736120/-/DCSupplemental.

Published November 6, 2023.

Understanding how plant photorespiration varies with environmental conditions requires measuring it in the modern and past. Photorespiration rates can be measured in real time using various techniques (20, 23–25). However, to our knowledge, all existing methods require living plants (23) or well-preserved dead specimens that retain structural carbohydrates (24, 26) or amino acids (25). Here, we propose, validate, and apply a unique potential proxy for plant-relative photorespiration rate based on the abundance of the multiply isotopically substituted ("clumped") isotopologue $^{13}CH_2D$ in methoxyl groups (CH_3–O–*R*) in wood lignin. Methoxyl groups (also termed methoxy groups) comprise about one in eight carbon atoms in lignin, a main biopolymer in wood. Lignin methoxyl groups are a major sink of one-carbon metabolic intermediates (termed C1 carbon) in trees (27–29) and can be preserved in the rock record for tens of millions of years (30). The stable hydrogen (δD) and carbon ($\delta^{13}C$) isotope compositions of wood methoxyl groups are established climate proxies (31–34) but clumped isotope compositions ($\Delta^{13}CH_2D$ and $\Delta^{12}CHD_2$; defined below) have yet to be systematically explored beyond initial method development (35).

We first describe the conceptual basis of using methoxyl clumping as a tracer of photorespiration. We then validate this proxy using results from samples grown over ranges in atmospheric [CO_2] (280–1000 ppm) and mean daytime growing season temperature (18–28 °C) without water limitation, both from laboratory growth experiments and the environment. Next, we apply this proxy to an expanded dataset of environmental samples spanning large ranges in space (11–65°N), time (~200 y into the past), growing season temperature (10–28 °C), and water availability. We observe global trends in relative photorespiration rate with temperature and water availability and discuss the implications of these findings for the response of GPP to climate in the present, future, and past.

Proposed Basis for an Isotopic Photorespiration Proxy in Wood

Lignin methoxyl groups are formed during monolignol biosynthesis (i.e., the synthesis of the monomers that are polymerized into lignin) via the transfer of an intact methyl group to an aromatic ring (Fig. 1). The transferred methyl group is derived from a tetrahydrofolate-bound (THF) methyl group, which is created via the addition of an H atom from NADH (27) to a methylene (CH_2) group that ultimately originates from the C3 carbon in serine. Serine in plants has two broad biosynthetic origins: it forms either during photorespiration or from 3-phosphoglycerate (3-PGA) via the glycolysis or phosphorylation pathways (36). This 3-PGA is itself a direct or indirect product of photosynthesis. Another potential origin for this methylene group is from formate, which is a degradative byproduct of glyoxylate oxidation during one of the initial steps of photorespiration (27). We do not further consider the formate pathway as it is thought to be a minor, secondary source of photorespiratory serine in leaves [~20%, (37)], and not transported in high concentrations through phloem to lignifying cells (38). Under this simplification, the methylene groups that supply two-thirds of the C–H bonds in methoxyl groups in lignin can be considered to be effectively derived either from photosynthesis or photorespiration.

Previous work indicates that these methylene groups from photorespiratory vs. photosynthetic origins have different carbon and hydrogen isotopic compositions (24, 25). The dependence of the hydrogen isotopic composition of stereochemically distinct hydrogens at the C6 position of glucose (a CH_2 group) on atmospheric [CO_2] has been interpreted to indicate that methylene groups

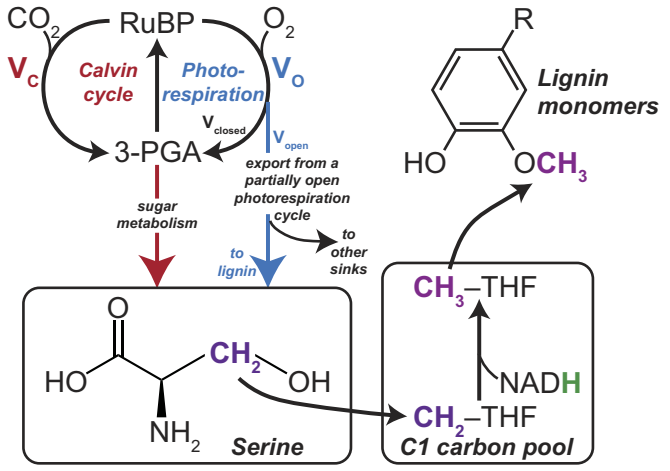

Fig. 1. Conceptual illustration of the premise behind using the isotopic composition of lignin methoxyl groups in wood as a proxy for relative photorespiration rates. The methoxyl group (O–CH_3) in lignin is derived from a methyl group bound to THF, which in turn is formed by the hydrogenation of a methylene group (CH_2) by NADH. The methylene group is derived from serine (27), which can be formed either during photorespiration or from products of the Calvin cycle (36). A third potential source—formate generated by the oxidation of photorespiratory glycolate—is thought to be minor (20%) and so we do not consider it in our conceptual model (27). We propose that serine methylene groups from these different origins have different clumped ^{13}C–D isotopic compositions [as has been suggested for δD and $\delta^{13}C$, (24, 25, 39, 40)] such that the isotopic composition of the plant C1 carbon pool will depend on the mixing fraction from these sources and lignin methoxyl groups will inherit this isotopic signal. The strength of this signal will depend to first order on the relative photorespiration rate (V_O/V_C) and the photorespiratory export fraction to lignin vs. other sinks. Abbreviations: RuBP, ribulose-1,5-biphosphate; 3-PGA, 3-phosphoglycerate; THF, tetrahydrofolate; NAD, nicotinamide adenine dinucleotide.

produced by photorespiration are hundreds of per mille (‰) lower in δD than the corresponding groups originating from the Calvin cycle (24, 39–41). The carbon isotope composition of the serine methylene group in leaves also depends on atmospheric [CO_2], which can be explained if these two sources differ in $\delta^{13}C$ by about 10‰ (25). Since lignin methoxyl groups inherit two-thirds of their C–H bonds from the methylene group in serine, we hypothesize that the isotopic compositions of lignin methoxyl groups will be sensitive to the relative contributions from serine methylene groups formed during photorespiration vs. from the products of photosynthesis and therefore could be used to track the relative amount of photorespiration in plants.

Importantly, this hypothesis requires that photorespiratory serine CH_2 groups made in photosynthesizing tissues are actually exported and used to form methoxyl groups in wood. We note that there are multiple potential carriers of the signal beyond serine such as such as glycine, CH_2–THF, or CH_3–THF. Here, we use serine as a catch-all term for these carriers and note that our hypothesis does not depend on which one is exported. The incorporation of the photorespiratory isotopic signal to lignin methoxyl groups could occur in one of two ways: what we term an "indirect" pathway through incorporation of this moiety into glucose, or a "direct" pathway whereby photorespiratory serine escapes recycling and is a source of lignin methoxyl groups. The indirect pathway works as follows: i) The methylene group in photorespiratory serine is first recycled through 3-PGA and contributes to the C6 position of glucose—this is the premise behind the glucose-C6-based photorespiration proxy discussed above (24); ii) this group is later used to make secondary serine from 3-PGA via the phosphorylation or glycolysis pathway and iii) is ultimately converted to a lignin methoxyl group in wood. We consider this pathway possible but potentially problematic because multiple enzymatic steps in sugar

metabolism downstream of initial glucose formation break and form C–H bonds in moieties that source the CH_2 group in 3-PGA, which may overprint the original isotopic signal of relative photorespiration rate (39, 42–44).

The direct pathway would arise from a photorespiration cycle that is not fully closed (45–48). Rather, some photorespiration-derived serine is exported from leaves, translocated to xylem, and used directly as a source for lignin methoxyl groups in wood (Fig. 1). A partially open photorespiration cycle, wherein glycine and serine are incompletely recycled back to 3-PGA, has been proposed to explain why plants photosynthesizing under a triose phosphate utilization (TPU) limitation (i.e., high light, high $[CO_2]$, low temperature) exhibit reversed sensitivities of CO_2 assimilation rate to changes in $[CO_2]$ and $[O_2]$ (45, 49). Even under ambient growing conditions, isotope labeling experiments have shown that photorespiratory glycine and serine are still incompletely recycled (48). Export of these metabolites from leaves to wood is also consistent with the observation that serine is an abundant component of phloem (38, 46, 50, 51) and the general understanding that photorespiratory serine is an important source of methyl groups to a variety of biomolecules including lignin (51, 52). It has even been proposed that the reason C4 plants lack significant woody tissue is because their photorespiration rates are too low to export enough C1 carbon units to support the major methoxyl sink of wood lignin (52).

Given this, we hypothesize that isotopic composition of wood methoxyl groups will depend on both the rate of photorespiration relative to carbon fixation and the fraction of serine (plus any other carriers of serine's CH_2 group) exported from the photorespiration pathway (hereafter, the photorespiratory export fraction) and used to make lignin methoxyl groups (Fig. 1). Changes to either parameter would result in changes in the mixing ratio of photorespiratory to photosynthetic serine sources in lignin. As described above, the controls on relative photorespiration rate are well-established (8, 10). Conversely, photorespiratory export fractions between 8 and 50% have been measured in the laboratory and have been proposed to depend on water stress and the availability or form of nitrogen and/or sulfur, but the controls on the fraction of photorespiratory serine exported specifically to lignin methoxyl groups are not understood (46–48, 52–54).

Clumped ^{13}C–D Compositions as a Tracer of Mixing. To test the hypothesis that the isotopic composition of lignin methoxyl groups can be used as a proxy for photorespiration rate, we use the measurement of the relative abundance of methoxyl groups with more than one rare isotope, termed clumped isotopologues [e.g., (55)] as a tracer of the relative contribution of photosynthetic vs. photorespiratory precursors to lignin methoxyl groups. In this specific case, the most abundant clumped isotopologue is $^{13}CH_2D$ (~5 ppm at natural abundance). The $^{13}CH_2D$ clumped isotope composition is reported using Δ notation (56):

$$\Delta^{13}CH_2D = \left(\frac{^{13}CH_2D R}{^{13}CH_2D R^*} - 1 \right) \times 1000 \qquad [1]$$

where $^{13}CH_2D R$ is the ratio of $[^{13}CH_2D]/[^{12}CH_3]$ and the * represents a random distribution of isotopes among all isotopologues.

In isotopically equilibrated systems, Δ values are solely functions of temperature (56) and therefore can be used for paleothermometry [e.g., (55)]. Our preliminary work on three wood samples demonstrated that lignin methoxyl $\Delta^{13}CH_2D$ values are not consistent with formation in internal isotopic equilibrium and instead must be controlled by nonequilibrium processes such as kinetic isotope effects expressed during C–H bond formation and mixing of different sources (35). Importantly for our purposes, models indicate that ^{13}C–D clumped isotopic compositions of kinetically controlled processes are not strongly affected by the $\delta^{13}C$ and δD values of the source elements but instead largely reflect differences in the kinetic isotope effects of the specific reactions that form and destroy C–H bonds (57). As such, we propose that if serine CH_2 groups formed during photorespiration vs. from Calvin cycle products have different degrees of ^{13}C–D clumping, lignin methoxyl groups will inherit these C–H bonds, and the lignin methoxyl $\Delta^{13}CH_2D$ value will depend on the relative contributions from each pathway, specifically the relative photorespiration rate and the photorespiratory export fraction to wood lignin. We estimate that the irreversible addition of the third hydrogen from NADH acts to decrease the total $\Delta^{13}CH_2D$ measurement range by ~17% relative to the range of ^{13}C–D clumping expected in precursor CH_2 groups (i.e., a scale compression; *SI Appendix*) but does not otherwise impact the value.

In contrast to our expectation for $\Delta^{13}CH_2D$, we note the same model predicts that the relative abundance of another clumped isotopologue that we routinely measure, $\Delta^{12}CHD_2$—see *SI Appendix* for details, is highly sensitive to the addition of the third hydrogen atom from NADH, due to its association with a large kinetic isotope effect (31, 34, 58, 59). This results in a so-called "combinatorial effect" in which the clumped isotope value is a function of both the kinetic isotope effect and the difference in hydrogen isotopic composition of the reactants [in this case the CH_2 group and the third hydrogen atom, (57)], which makes interpretation of D_2-bearing isotopologues more complex as compared to ^{13}C–D counterparts. This is described quantitatively in *SI Appendix*. Based on this, we focus on $\Delta^{13}CH_2D$ as a tracer of photorespiration.

Validation of the Clumped Isotopic Photorespiration Proxy in Wood

To test whether methoxyl $\Delta^{13}CH_2D$ values are sensitive to relative photorespiration rates as proposed above, we analyzed samples where only one of two parameters that controls these rates (atmospheric $[CO_2]$ and temperature) varied significantly. Here, we only used specimens from water-replete environments as water limitation can modify the photorespiratory export fraction (47) and the CO_2 concentration inside the leaf (c_i) independent of atmospheric $[CO_2]$ due to changes in stomatal conductance (60). In the next section, we present data on water-limited samples but restrict our discussion here to these simpler water-replete samples to focus on the roles of temperature and atmospheric $[CO_2]$.

The Effect of Temperature on Methoxyl Clumping. We first examine wood samples from trees grown in similar atmospheric $[CO_2]$ but different mean growing season temperatures. The relative photorespiration rate, which we define specifically as the rate of oxygenation by Rubisco (V_O, which initiates photorespiration) to carboxylation (V_C, which initiates carbon fixation), increases with temperature. For example, in an atmosphere with 300 ppm $[CO_2]$, a standard model of photosynthesis predicts that V_O/V_C should roughly double between 20 °C and 30 °C [(8, 10, 20); see *Materials and Methods* and *SI Appendix*, Fig. S13 for details). We therefore tested whether growth temperature affects $\Delta^{13}CH_2D$ values by examining wood from 5 trees across a range of climates (18–28 °C mean daytime growing season temperature; Fig. 2*A*; see *Materials and Methods* for explanation of growing season temperature calculation). We isolated any temperature signal from historical variations in $[CO_2]$ by using wood from samples that all grew prior to 1950 but are at most a few hundred years old,

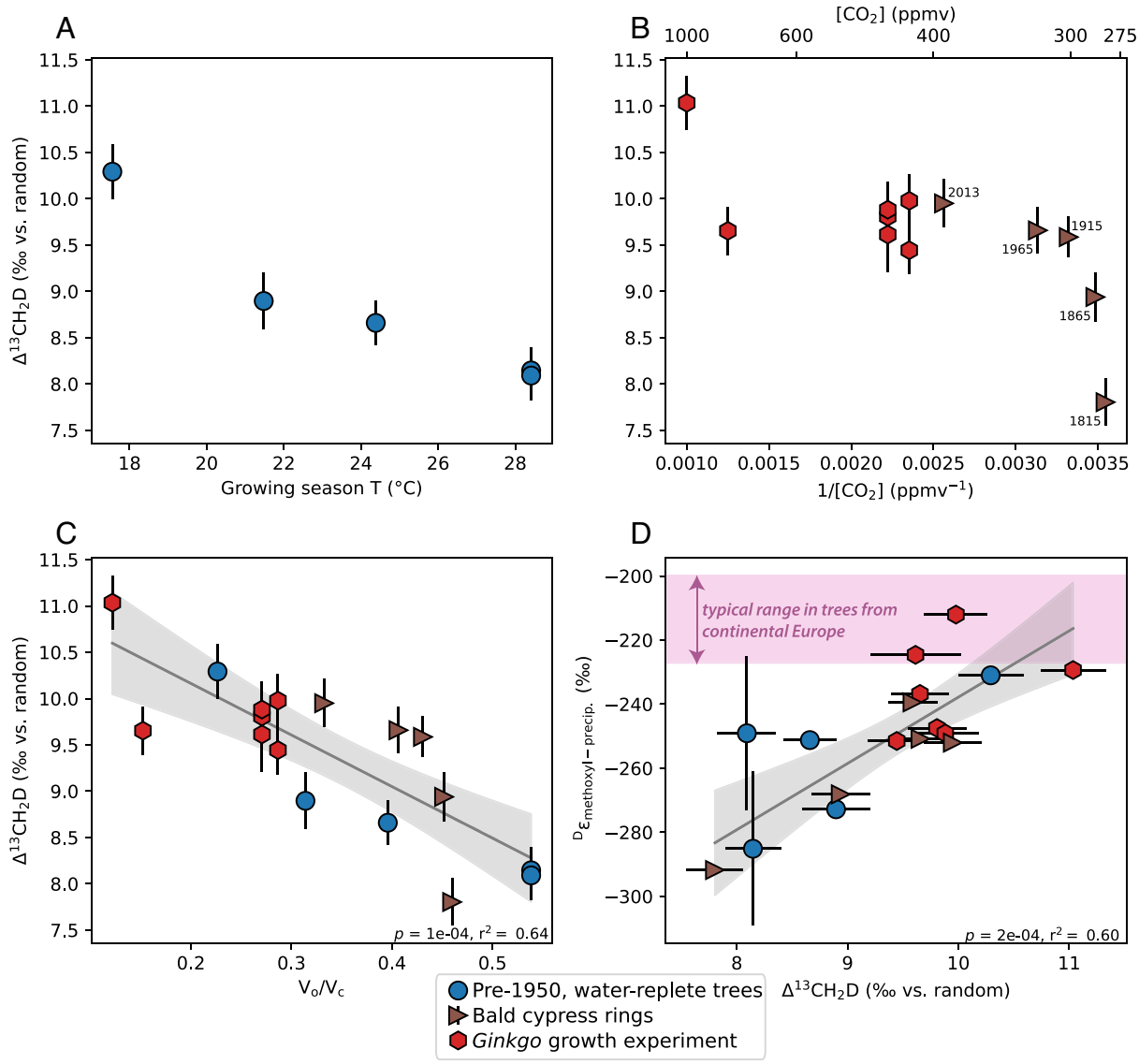

Fig. 2. Methoxyl $\Delta^{13}CH_2D$ depends on atmospheric $[CO_2]$ and temperature in trees growing in water-replete environments. (*A*) Wood methoxyl $\Delta^{13}CH_2D$ vs. mean daytime temperature during the growing season for trees grown without water limitation (water-replete). All trees were harvested before 1950. (*B*) Wood methoxyl $\Delta^{13}CH_2D$ vs. 1/atmospheric $[CO_2]$ for *Ginkgo biloba* from *Ginkgo* growth experiments (red hexagons) and from a 200-y longitudinal study of a living *Taxodium dis.* tree (brown triangles). Each bald cypress sample comprises 10 or 15 consecutive years of growth; average year listed next to each point. (*C*) All data from (*A*) and (*B*) plotted vs. estimated V_O/V_C (relative photorespiration rate)—see *Materials and Methods* for details of the calculation. Data in (*B*) are shown vs. 1/$[CO_2]$ because V_O/V_C is expected to linearly depend on this variable. (*D*) Hydrogen isotopic composition of methoxyl groups normalized to the δD of mean annual precipitation ($^D\varepsilon_{methoxyl-precip.}$) vs. $\Delta^{13}CH_2D$. Pink box is the average ±1SD of $^D\varepsilon_{methoxyl-precip.}$ given in previous studies of continental Europe (n = 104, see refs. 31, 34, and 58). Note this range has been adjusted for an interlaboratory offset in methoxyl δD scales (35). Error bars are ±1SE of measurement error for $\Delta^{13}CH_2D$, and ±95%CI of the δD of mean annual precipitation for $^D\varepsilon_{methoxyl-precip.}$ value. Gray lines are error-weighted linear fits and associated ±95%CI to data.

such that $[CO_2]$ was restricted to between 290 and 310 ppm (see *SI Appendix* for details).

We observe that $\Delta^{13}CH_2D$ values of these samples decrease in a roughly linear manner with increasing temperature from 10.3‰ at 18 °C to 8.1‰ at 28 °C (Fig. 2*A* and *SI Appendix*, Table S4). Although $\Delta^{13}CH_2D$ for equilibrated systems also depends inversely on temperature, this signal cannot arise from an equilibrium isotope effect for three reasons (*SI Appendix*, Fig. S3): i) The values are too high by 2 to 4‰ compared to equilibrium at these growth temperatures, ii) the ~2‰ range is 6× larger than predicted for a ~10 °C range in growth temperature, and iii) the $\Delta^{12}CHD_2$ values in the same samples (and all woods measured so far) are <0‰ but highly variable (–15‰ to –60‰), which is inconsistent with internal isotopic equilibrium at any temperature (35). Instead, we conclude that the clumped isotopic compositions of these wood methoxyl groups are controlled by mixing of sources with different $\Delta^{13}CH_2D$ values such that the mixing ratio correlates with temperature. The negative, highly variable $\Delta^{12}CHD_2$ values are also consistent a conceptual model where a third hydrogen with a large, variable kinetic isotope effect is added to a pool of CH_2 groups with multiple sources (see *SI Appendix* for details). Both datasets are thus consistent with a control based on relative photorespiration rate.

The Effect of $[CO_2]$ on Methoxyl Clumping. Relative photorespiration rates (V_O/V_C) also vary inversely with $[CO_2]$ when atmospheric $[O_2]$ is fixed. Specifically, V_O/V_C ~linearly increases with 1/$[CO_2]$ and is thus more sensitive to a change in $[CO_2]$ at lower absolute $[CO_2]$ values (10). For example, again according to the standard photosynthesis model described above, the decrease in V_O/V_C from 300 to 400 ppm $[CO_2]$ is roughly equivalent to the decrease in V_O/V_C from 600 to 1,000 ppm (*SI Appendix*, Fig. S13). Given this, we hypothesize that $\Delta^{13}CH_2D$ values will be most

sensitive to changes in $[CO_2]$ at lower starting atmospheric $[CO_2]$. On this basis, we analyzed tree rings spanning 200 years (~1810 to 2019 CE) from a single living bald cypress (*Taxodium distichum*) tree grown in standing water in S. Florida that captures the rise in atmospheric $[CO_2]$ from preindustrial (~280) to modern (~400 ppm) levels while atmospheric $[O_2]$ was effectively constant [e.g., (61)].

For these samples, $\Delta^{13}CH_2D$ values increase with time (and thus $[CO_2]$), from 7.80 ± 0.26‰ (1SE) in 1810–1819 to 9.95 ± 0.25‰ (1SE) in 2005–2019 (*SI Appendix*, Table S6) and with intermediate values in between (Fig. 2*B*). These methoxyl $\Delta^{13}CH_2D$ values exhibit a nonlinear relationship with atmospheric $[CO_2]$ such that most of the increase occurs as $[CO_2]$ increases from ~280 to 320 ppm (a 1.6‰ increase and thus ~6× 1SE measurement precision).

We further test the dependence of $\Delta^{13}CH_2D$ on $[CO_2]$ by measuring methoxyl groups from basal root shoots of *Ginkgo biloba* trees grown in both ambient and elevated atmospheric $[CO_2]$ treatments (425, 450, 800, or 1,000 ppm) in open-top chambers from the Fossil Atmospheres project [(62); *Materials and Methods*]. We used basal root shoots from this *Ginkgo* growth experiment that grew in 2020, by which point trees had grown in and acclimated to a given $[CO_2]$ treatment for 4 y. These trees maintained a constant c_i/atmospheric $[CO_2]$ in the growth year prior to sampling regardless of $[CO_2]$ treatment (62), and therefore we assume that c_i directly varies with a chamber's $[CO_2]$. From 425 to 800 ppm $[CO_2]$, root shoot $\Delta^{13}CH_2D$ values are indistinguishable from the bald cypress data at $[CO_2]$ > 300 ppm: 9.68 ± 0.08‰ (1SE, n = 5, ginkgo) vs. 9.73 ± 0.11‰ (n = 3, bald cypress) (Fig. 2*B*). The sample grown at 1,000 ppm has a more elevated $\Delta^{13}CH_2D$ value of 11.05 ± 0.29‰ (1SE). These experiments support the bald cypress data indicating that $\Delta^{13}CH_2D$ is a nonlinear and monotonically increasing function of atmospheric $[CO_2]$ with a larger rate of change in $\Delta^{13}CH_2D$ vs. $[CO_2]$ at lower $[CO_2]$.

A Combined Reference Frame of V_O/V_C. Combining and summarizing these results, we find that in water-replete conditions, $\Delta^{13}CH_2D$ values decrease as either temperature increases or $[CO_2]$ decreases. Both variables positively correlate with an increasing relative photorespiration rate. This general relationship can be observed by comparing $\Delta^{13}CH_2D$ to an estimate of relative photorespiration rate (V_O/V_C) for each sample using a standard model of photosynthesis (Fig. 2*C*; see *Materials and Methods* for model details). In doing this calculation, we make a series of assumptions including that all trees studied share the same photosynthetic model parameters and that there is a universal, temperature-dependent scaling factor between c_i and atmospheric $[CO_2]$ (10). We observe that all three datasets form an overlapping linear relationship in terms of $\Delta^{13}CH_2D$ vs. V_O/V_C (P < 1e-4, r^2 = 0.64; Fig. 2*C*). We also compared this result to the predictions of a more complex model that incorporates acclimation of photosynthetic parameters and c_i/atmospheric $[CO_2]$ to a plant's growing environment [*P*-model v.1.0, (63, 64)]. This yields qualitatively similar results: The range of predicted V_O/V_C values is compressed but the linear relationship between $\Delta^{13}CH_2D$ and V_O/V_C persists (P < 1e-3, r^2 = 0.54; see *SI Appendix*, Fig. S11). We interpret this result to indicate that the specific V_O/V_C values shown in Fig. 2*C* are uncertain, but the dependence of $\Delta^{13}CH_2D$ on relative changes in V_O/V_C is a robust result. Based on this and the associated theoretical basis discussed above, we proceed with the hypothesis that wood methoxyl $\Delta^{13}CH_2D$ values track and linearly correlate with (at least to first order) relative photorespiration rates in water-replete plants. Importantly, this also requires that in these samples, the photorespiratory export fraction to lignin is constant or proportional to relative photorespiration rate.

Test of the Dependence of $\Delta^{13}CH_2D$ on Relative Photorespiration Rates. We further test the hypothesis that $\Delta^{13}CH_2D$ depends on relative photorespiration rate using the methoxyl hydrogen isotopic composition (δD vs. VSMOW) of the same samples described above. As discussed, prior work indicates that the methylene group formed during photorespiration is lower in δD than the equivalent group derived from photosynthate (i.e., Calvin-cycle derived) (24, 39–41). This sets up a prediction that can test our hypothesis: If the low $\Delta^{13}CH_2D$ values (<9‰) do indeed reflect an increased contribution of photorespiratory serine methylene groups to lignin methoxyl groups, then all else being equal, these methoxyl groups would also be lower in δD compared to samples with elevated $\Delta^{13}CH_2D$ (31, 34, 58, 59). To apply this test, we normalize wood methoxyl δD values to the hydrogen isotopic composition of local precipitation, the source of hydrogen in a plant (31, 34): ${}^{D}\varepsilon_{methoxyl\text{-}precip.} = 1000 \times ((\delta D_{methoxyl}+1000)/(\delta D_{precip.}+1000) - 1)$. Following previous work (31, 34, 58), we estimate $\delta D_{precip.}$ for each sample using a model (65, 66) based on sample location and elevation, assuming that the hydrogen isotopic composition of mean annual precipitation approximates that of plant water during the growing season and has not changed substantially in the past few hundred years (i.e., the age range of the samples). We observe a positive, linear relationship between ${}^{D}\varepsilon_{methoxyl\text{-}precip.}$ and $\Delta^{13}CH_2D$ for the samples discussed above (Fig. 2*D*), which is consistent with our prediction that decreasing $\Delta^{13}CH_2D$ reflects an increasing contribution of photorespiratory material to lignin methoxyl groups. As such, this comparison provides independent support for our hypothesis that the isotopic composition of methoxyl groups vary in their δD values and by extension C–H bond ordering as a function of climatic variables (T and atmospheric $[CO_2]$) that are expected to correlate with relative photorespiration rate.

On this basis, we propose that $\Delta^{13}CH_2D$ values in wood can be used to reconstruct (semiquantitatively) relative photorespiration rates both from modern and ancient specimens with preserved lignin, provided photorespiratory export fraction to lignin remains approximately constant or proportional to V_O/V_C. The same is true, by extension, of ${}^{D}\varepsilon_{methoxyl\text{-}precip.}$ if the δD value of plant water is independently known or determinable (e.g., by analyzing the nonexchangeable δD of cellulose or whole-wood in the same sample).

Global Trends in Wood Methoxyl Clumping

We now present analyses of the isotopic composition of wood methoxyl groups from an additional 17 trees grown around the world with varying water status. All samples are from wood formed before 1950 and the associated inflection in the rate of atmospheric $[CO_2]$ increase (67) (see *SI Appendix*, Fig. S1 for locations), thus allowing us to control for atmospheric $[CO_2]$ (~290 to 310 ppm). This expanded dataset (*SI Appendix*, Tables S1–S4) includes the water-replete trees from the temperature test discussed above (n = 5), and the bald cypress ring sets from before 1950 (n = 3), for a total sample size of 25. This comparison allows us to examine the role of water availability in setting $\Delta^{13}CH_2D$ values across a range of climates.

We observe that methoxyl clumping varies in characteristic ways vs. climate (Fig. 3*A*). In colder climates with estimated daytime growing season temperatures below 18 °C, all measured methoxyl $\Delta^{13}CH_2D$ values fall within a narrow range of 9.3 and 10.4‰. The SD of these samples (n = 10; 0.35‰, 1SD) is similar to the

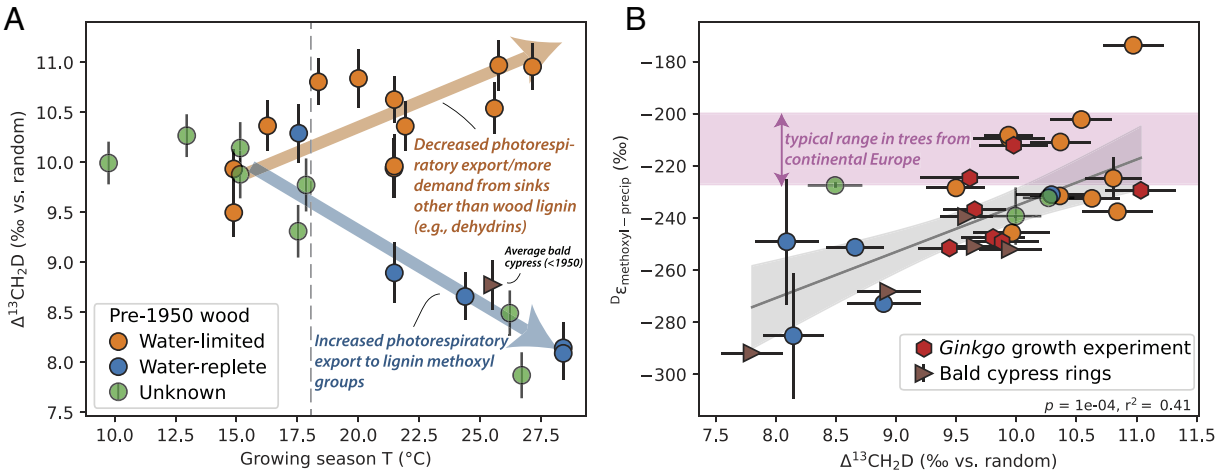

Fig. 3. (*A*) Wood methoxyl $\Delta^{13}CH_2D$ vs. mean growing season daytime temperature for all wood formed before 1950 in the global compilation. Samples colored based on a categorization of water availability (replete, limited, or unknown; see *Materials and Methods* for details). Colored arrows illustrate our interpretation of the observed trends in water-limited vs. water-replete trees. Dashed gray line denotes 18°C, above which quantitatively different behavior is observed in water-limited vs. water-replete trees. Bald cypress data point is the average of three time periods before 1950, to allow comparison to the other data on this plot. (*B*) Relationship between $\Delta^{13}CH_2D$ value and the isotopic difference between measured methoxyl hydrogen isotopic composition and mean annual precipitation ($^{D}\varepsilon_{methoxyl-precip.}$) among all samples measured in study (including those formed after 1950, and the *Ginkgo* growth experiment). Legend in (*A*) also applies to (*B*). The gray line is the error-weighted linear regression along with the ±95%CI of the fit. The pink box is the average ±1SD of $^{D}\varepsilon_{methoxyl-precip.}$ from previous studies of continental Europe (n = 104, see refs. 31, 34, 58), adjusted for the interlaboratory offset in methoxyl δD scales (35). Error bars are ±1SE of measurement error for $\Delta^{13}CH_2D$ and ±95%CI of δD of mean annual precipitation for $^{D}\varepsilon_{methoxyl-precip.}$ values.

typical error of a single measurement (0.25‰, 1SE), and so we consider these $\Delta^{13}CH_2D$ values effectively indistinguishable from each other. At temperatures above 18 °C, the range of methoxyl $\Delta^{13}CH_2D$ expands with increasing temperature to values as low as 7.9‰ and as high as 11.0‰ (n = 15).

As noted above, these trends cannot be a result of differences in $[CO_2]$ as it is largely invariant over the study interval (290–310 ppm). The trends are also not controlled by how the mean growing season temperature is estimated provided it is done consistently for all samples (*SI Appendix*, Fig. S12). In *SI Appendix*, we examine and rule out a variety of other potential origins for the first-order trends in $\Delta^{13}CH_2D$ values, including plant type (e.g., gymnosperm vs. angiosperm), wood composition (e.g., methoxyl concentration, earlywood vs. latewood), and climate parameters other than temperature (e.g., light intensity, relative humidity).

Instead, we find that the parameter that best relates to whether $\Delta^{13}CH_2D$ values tend to increase or decrease at higher temperatures (>18 °C) is the water availability in a plant's growing environment. We define water availability as follows (see *Materials and Methods* for details): Trees that grew in a water-replete environment (e.g., in a swamp or in a state of constant soil moisture saturation during the growing season) are assigned a binary water limitation value of 0. Trees that appear water limited (e.g., grown on well-drained soils or steep slopes) are assigned a binary water limitation of 1. Samples lacking environmental information are labeled "unknown." We tested these assignments using cellulose $\delta^{13}C$ and $\delta^{18}O$ data of the same samples: Water-replete samples tend to have lower $\delta^{13}C$ values and lower $\delta^{18}O$ values (once corrected for the $\delta^{18}O$ of precipitation) compared to water-limited samples, which agrees with expectations given the first-order controls on these variables (see *SI Appendix* for details). This description of water limitation is a simplification, but one that we find useful for the initial examination of the data.

Trees that are not limited by water during growth tend to decrease in $\Delta^{13}CH_2D$ as mean daytime growing season temperature increases above 18 °C, while trees growing above 18 °C that are water-limited yield $\Delta^{13}CH_2D$ values that are similar to or higher than those grown below 18 °C. Trees with unknown water availability can adhere to either trend. These groupings are statistically significant at the 95% level: $\Delta^{13}CH_2D$ values of water-limited trees growing above 18 °C are significantly different from water-replete trees growing above 18 °C (P < 1e-5, Welch's t test), and both groups are resolved from the population of $\Delta^{13}CH_2D$ values for trees that grew below 18 °C (P < 0.03 and P < 1e-3, respectively, Welch's t test).

Analogous trends for $\Delta^{13}CH_2D$ vs. climate are seen for $^{D}\varepsilon_{methoxyl-precip.}$, although departures from the cold-climate average are only visually apparent above 20 °C (*SI Appendix*, Fig. S2). Below 20 °C, $^{D}\varepsilon_{methoxyl-precip.}$ values are consistent with the average observed from prior studies of wood from continental Europe [about –213 ± 18‰ (1SD, n = 104), refs. 31, 34, 35, and 5, see *SI Appendix* for details]—our measured data from cooler climates all fall within 15‰ of this mean value regardless of water availability. Above 20 °C, samples diverge from this mean value by up to +40‰ and down to –72‰ and also group by water availability (*SI Appendix*, Fig. S2). As such, a correlation between $^{D}\varepsilon_{methoxyl-precip.}$ and $\Delta^{13}CH_2D$ persists over an expanded range of values, where the highest values of both variables are exclusively seen in trees that grew under water limitation (P = 1e-4, r^2 = 0.41; Fig. 3*B*). We considered whether changes in $^{D}\varepsilon_{methoxyl-precip.}$ with water availability could also be due to varying degrees of evaporative isotopic enrichment in leaf water vs. xylem water and found that that only about 25 to 50% of the correlation between $^{D}\varepsilon_{methoxyl-precip.}$ and $\Delta^{13}CH_2D$ in this expanded dataset could be due to variation in leaf water evaporative enrichments (see *SI Appendix* for details). As such, we interpret the correlation between $^{D}\varepsilon_{methoxyl-precip.}$ and $\Delta^{13}CH_2D$ as further evidence that both variables are tracking mixing ratios of photorespiratory to photosynthetic methylene groups.

Divergent Responses to Increasing Photorespiration Rates with Temperature as a Function of Water Availability

Photorespiration is estimated to be ~25% the rate of photosynthesis in C_3 plants at 25 °C and ~350 ppm atmospheric $[CO_2]$, but the extent to which individual plants in a given environment

depart from this value is generally not known (19, 20). We interpret the results from the global dataset to indicate that the fluxes of photorespiratory metabolites to wood change with increasing growing season temperature and that the direction of this change depends on water availability. We now propose explanations for these results.

Similar Relative Photorespiration Rates in Cooler Climates. At low growth temperatures (<18 °C), $\Delta^{13}CH_2D$ and ${}^{D}\varepsilon_{methoxyl–precip.}$ values appear insensitive to growing season climate, which we interpret to indicate that the relative contribution of photorespiratory vs. photosynthetic serine to lignin methoxyl groups is itself insensitive to environmental conditions. We consider two complementary explanations for this observation. First, it is possible that relative photorespiration rates are less sensitive to temperature at low temperatures. For example, at a constant $[CO_2]$ of 300 ppm and using the standard model for V_O/V_C described above that employs universal Rubisco kinetic parameters, V_O/V_C is about half as sensitive to a 3 °C change in temperature from 15 to 18 °C as compared to 22 to 25 °C (*SI Appendix*, Fig. S13). However, the more complex *P*-model described above predicts that the sensitivity of V_O/V_C to temperature is more similar over these temperature ranges, although still slightly nonlinear (*SI Appendix*, Fig. S13). If the predictions of the *P*-model are more accurate, it suggests that this explanation is less likely.

Second, plants in boreal to temperate climates exhibit some degree of convergence in assimilation-weighted photosynthesis temperature that is not incorporated into our estimates of daytime growing season temperature [e.g., (68, 69)]; i.e., plants in cooler climates tend to preferentially assimilate more carbon during the warmer parts of the day. Thus, the true mean photosynthesis temperatures of our samples from boreal climates, when weighted by assimilation rate at the scale of minutes or hours, are likely higher and more similar to those of temperate climates than what our mean monthly climate models predict. This would make V_O/V_C values, and thus $\Delta^{13}CH_2D$ and ${}^{D}\varepsilon_{methoxyl–precip.}$ values, more similar across a range of climates. This explanation is supported by existing evidence that ${}^{D}\varepsilon_{methoxyl–precip.}$ values are insensitive to temperature across all but the warmest climates in continental Europe [n = 104, (31, 34, 58)].

Positive Correlation between Relative Photorespiration Rate and Temperature in Water-replete Trees. With increasing temperature, plants growing in water-replete conditions exhibit decreasing $\Delta^{13}CH_2D$ and ${}^{D}\varepsilon_{methoxyl–precip.}$ values. This can be explained as follows: Plants with less water limitation can afford to transpire more (9, 60), maintain higher stomatal conductance and higher assimilation rates as temperatures increase, and thus photosynthesize at a higher temperature on average. If the photorespiratory export fraction to lignin remains constant or increases, then as temperature increases so will V_O/V_C and the relative contribution of photorespiratory serine to lignin methoxyl groups (Fig. 3*A*).

No Correlation or Negative Correlation between Photorespiratory Export and Temperature in Water-limited Trees. Among trees with some degree of water limitation, we observed that as temperatures increase above 18 °C, $\Delta^{13}CH_2D$ and ${}^{D}\varepsilon_{methoxyl–precip.}$ values either do not change or increase compared to samples grown at lower temperatures (Fig. 3*A*). The maximum $\Delta^{13}CH_2D$ values observed in this subset of data are 11‰, which is similar to the maximum value measured in the *Ginkgo* growth experiment at 1,000 ppm $[CO_2]$. At this high $[CO_2]$, V_O/V_C is likely <0.1 (*SI Appendix*, Fig. S13), and thus, we assume a $\Delta^{13}CH_2D$ value of ~11‰ approaches the pure photosynthetic endmember.

We considered two ways to explain this relationship as a consequence of how water-limited plants respond to high temperatures. We first considered whether it could be the result of a midday depression (sometimes termed the diurnal depression), wherein plants in hot climates reduce stomatal conductance and assimilate less carbon during the hottest parts of the day (70–72). If this occurred in the trees studied, it would act to lower the assimilation-weighted mean photosynthesis temperature (and thus the average V_O/V_C) compared to the average daytime growing season temperature we calculated using climate data alone. As this phenomenon is chiefly driven by vapor pressure deficit (71), the midday depression tends to increase with increasing water limitation (73) and would be more apparent in water-limited trees.

To test this idea quantitatively, we calculated differences between average daytime temperature and assimilation-weighted temperature using previously published datasets from hot climates where a midday depression in assimilation rate was observed (*SI Appendix*, Table S8). We found that reduced assimilation during the midday depression can indeed lower average growth temperatures in hot, water-limited plants, but only by up to 2 °C vs. ambient temperature and vs. water-replete plants from the same climates (see *SI Appendix* for details). This 2 °C difference is too small to be the only explanation for similar $\Delta^{13}CH_2D$ values in samples with average temperatures between 18 and 28 °C. It also can only explain why $\Delta^{13}CH_2D$ values from water-limited plants would not decrease with increasing environmental temperature, and cannot explain why $\Delta^{13}CH_2D$ values in some samples increase from ~10‰ to ~11‰ over the same temperature range, which suggests a dominantly photosynthetic source to lignin methoxyl groups despite an increasing V_O/V_C. We thus consider midday depressions to play a minor role in setting the $\Delta^{13}CH_2D$ values of water-limited systems and turn to another explanation.

Instead, we propose that the $\Delta^{13}CH_2D$ data reflect an increase in alternative sinks for photorespiratory serine (and associated intermediates) at elevated temperatures under water-limited conditions in hot climates. Such additional sinks would act to reduce the photorespiratory export fraction to lignin methoxyl groups. For example, some plants growing under water-limited conditions produce glycine and serine-rich dehydrin proteins, which help plants retain water (reviewed in ref. 74). A ^{13}C labeling experiment showed that in a water-stressed soybean (*Glycine max*) leaf under low-CO_2 conditions, nearly all photorespiratory glycine was routed to leaf proteins to mitigate water loss instead of being used to make photorespiratory serine (75). If a similar response occurs in trees under water stress, then lignin methoxyl groups would acquire an increasing relative flux from photosynthate even as V_O/V_C increases as the photorespiratory precursors would be shunted elsewhere. Put another way, plants growing under hot, water-limited conditions may photorespire more, but also export fewer photorespiratory metabolites to lignin. Alternatively, hot, water-limited trees with low stomatal conductance could reduce the photorespiratory export fraction altogether. Specifically, a lower photorespiratory export fraction may be advantageous when chloroplasts are supply-limited (i.e., low CO_2 input) (47, 76). Either mechanism could reduce photorespiratory serine fluxes to lignin methoxyl groups and result in invariant or increasing wood methoxyl $\Delta^{13}CH_2D$ (and ${}^{D}\varepsilon_{methoxyl–precip.}$) values with increasing temperature.

This explanation is supported by existing isotopic data from wood methoxyl groups: tropical plants with saline water sources (e.g., mangroves) have higher ${}^{D}\varepsilon_{methoxyl–precip.}$ values than nearby trees without salinity stress (33). This can be explained if tropical plants with saline water sources use more photorespiratory serine and glycine to make dehydrins than those with fresh water, and thus wood methoxyl δD values of plants with saline water are

higher than freshwater counterparts even if the δD of the water sources are similar, which agrees with observations (33). A key next step to test this proposal would be to independently model photorespiratory export fraction to lignin vs. to other sinks as a function of environmental conditions (e.g., temperature, $[CO_2]$, and water availability) and compare these predictions to samples as we did for V_O/V_C with the water-replete samples above (Fig. 2*C*). However, this is not yet possible because, unlike with Rubisco kinetics, the environmental controls on photorespiratory export fractions are not sufficiently understood (47, 48, 52).

Implications for Relative Photorespiration Rates in the Near-future and Considerations for Reconstruction in the Past

The Effect of Photorespiration on GPP in Near-future Climates. With respect to the carbon budget of photosynthesis alone, photorespiration is considered deleterious to assimilation and a key limit on GPP (8, 77). As a result, rising atmospheric $[CO_2]$ in the near future is expected to suppress relative photorespiration rates, which will contribute to an increase GPP (often termed the CO_2 fertilization effect) and therefore mitigate a portion of the anthropogenic rise in $[CO_2]$, even after accounting for the concomitant increase in global temperature (3, 78, 79). Such a suppression in relative photorespiration rate has been observed in some cultivated crops (24) and peat mosses (26), is supported by the bald cypress sample examined here (Fig. 2*B*), and has been proposed to have contributed to the ~30% rise in GPP over the Industrial Era (80, 81). However, photorespiration has benefits to plant growth beyond a strict accounting of photosynthetic carbon assimilation. For instance, photorespiration can protect plants from excess photooxidation (17, 82, 83) and promote important metabolic processes including nitrogen assimilation, sulfur cycling, and wood production (18, 46, 47, 84). It is therefore not obvious that further suppression of photorespiration globally through rising atmospheric $[CO_2]$ will necessarily increase the terrestrial carbon sink.

Our data contribute to this issue as follows. We interpreted the invariant $\Delta^{13}CH_2D$ data from cooler climates (<18 °C) to indicate that relative photorespiration rates are low overall ($V_O/V_C < 0.25$) and less sensitive to environmental temperature and water stress. This suggests that further gains in carbon assimilation rate associated specifically with the suppression of photorespiration—i.e., by lowering V_O—would be marginal in these environments. Instead, other factors may matter more for determining the effects of climate change on GPP, such as the direct effect of increasing $[CO_2]$ on increasing V_C (81), the ability of individual species to acclimate to rising temperatures (85, 86), and the extent of nutrient limitation (87), which could in fact be exacerbated by the suppression of photorespiration-associated nitrate assimilation (47, 84, 88). However, as these systems continue to increase in temperature, other changes to photorespiration that emerge at higher V_O/V_C values may matter as discussed below.

The $\Delta^{13}CH_2D$ data indicated that relative photorespiration rates do increase with temperature above ~18 °C but that trees appear to adjust the apportionment of photorespiratory metabolites depending on water availability. We interpreted the decreasing $\Delta^{13}CH_2D$ data vs. temperature from water-replete systems to indicate that as V_O/V_C increases, more photorespiratory serine is exported and used in lignin methoxyl formation vs. serine from photosynthate. This maintenance or increase in the photorespiratory export fraction suggests that, here, the need to close the photorespiration cycle to recover 3-PGA is balanced or outweighed by the benefits of exporting these metabolites to lignin production (18, 46, 47). One implication of this is that photorespiratory carbon loss is not limiting assimilation in these samples. If so, we speculate that suppression of photorespiration due to rising $[CO_2]$ may not necessarily stimulate additional growth in similar systems. If correct, this could help explain why the Industrial Era rise in $[CO_2]$ has not consistently increased biomass production in individual trees in tropical climates based on tree ring width analyses (89).

In contrast, we interpreted the constant or increasing $\Delta^{13}CH_2D$ data vs. temperature from water-limited systems to indicate that as environmental temperature increases, water-limited trees respond by either reducing the photorespiratory export fraction and/or increasing the export of photorespiratory intermediates to systems that mitigate water stress like dehydrin proteins. The $\Delta^{13}CH_2D$ proxy cannot distinguish between these responses and a single response need not be shared by all trees studied. We expect that whether suppressing photorespiration with increasing $[CO_2]$ will or will not increase GPP in systems that are already hot and water-limited may depend on which response dominates. Plants from these environments that do not rely on the use of photorespiratory metabolites for water stress management may respond positively to rising $[CO_2]$ by reducing V_O/V_C and thus allowing for either increased photosynthetic capacity or increased water use efficiency. Such increases in GPP have been observed in some tropical forests over recent decades and in some large-scale free-air carbon enrichment experiments (81, 88, 90). However, in other tropical forests, increases in biomass production have been chiefly due to increasing dry season rainfall, not rising $[CO_2]$ (91). Hot, water-limited plants that have a high photorespiratory export fraction to molecules that mitigate water stress will not necessarily benefit—and could in fact be harmed—by suppressing photorespiration due to increasing $[CO_2]$ if this reduces their ability to manage water stress. For example, genetic mutants of the model plant *Arabidopsis thaliana* that lack a functional photorespiration cycle are less adept than the wild type at acclimating to conditions simulating drought stress (92). Given that rising vapor pressure deficits are increasing the fraction of plants facing water limitation worldwide (93, 94), understanding how photorespiration affects water-stressed plants, whether positive or negative, will only become more important in the near-future.

Potential for Reconstructions of Past Relative Photorespiration Rates. We have proposed a semiquantitative proxy for relative photorespiration rates and associated export fraction based on the clumped and stable hydrogen isotopic composition of methoxyl groups in wood. This method opens the possibility of reconstructing past relative photorespiration rates using fossil wood. Here, we close with considerations of the application of this proxy to ancient samples.

Wood methoxyl groups have been recovered from ancient tree rings from as far back as the early Eocene (55 Ma) and their hydrogen isotopic compositions used for paleoclimate reconstruction (30, 34, 95–97). These and other well-preserved samples should enable analysis and interpretation of the clumped isotopic composition of methoxyl groups over tens of millions of years. On these timescales, atmospheric $[CO_2]$ and, to a lesser extent, $[O_2]$ have varied from their present values (1), which would have driven global changes in V_O/V_C that this proxy could test for. Although degradation and alteration of $\Delta^{13}CH_2D$ signals is possible in ancient samples, methoxyl abundances, $\delta^{13}C$ values (29), and $\Delta^{12}CHD_2$ values can likely be used to monitor and screen for such effects (*SI Appendix*).

The response of this proxy to global climate variables appears to also depend on local factors, chiefly water availability. Thus, interpretation of the clumped isotopic composition of ancient

samples may be most useful when applied to fossils for which there is sedimentological evidence of the specific environment in which the tree grew. If information on the ancient environment is lacking, it may be possible to use other isotopic systems such as cellulose $\delta^{13}C$ and $\delta^{18}O$ to estimate carbon and water limitation.

Provided samples can be screened for diagenesis and placed in environmental context, example timeframes of interest include the Last Glacial Maximum, when both atmospheric [CO_2] and global mean temperatures were lower, and prior work has argued that plants were effectively starving due to excessive photorespiration (98, 99). Further back in the early Neogene and Paleogene, atmospheric [CO_2] and global temperatures were substantially higher than today, and prior work has proposed that a decrease in [CO_2] over this interval caused photorespiration to rise in C3 plants, slowing growth and silicate weathering rates, which stabilized [CO_2] at lower values (100) and potentially provided evolutionary pressure to develop the C4 and CAM pathways (19). These hypotheses implicate major differences in plant photorespiration rates at these times that may be testable with this technique. Such applications are clear next steps enabled by the proxy developed here.

Conclusions

Plant photorespiration is a key control on the gross primary productivity (GPP) of the terrestrial biosphere. The rate of photorespiration depends on temperature and atmospheric [CO_2], and therefore, relative photorespiration rates are expected to vary across both space and time. Tests of these concepts have been limited because it is challenging to directly measure photorespiration rates outside of the laboratory and in ancient samples. Here, we have proposed, validated, and applied a proxy for relative photorespiration rate based on the isotopic composition of wood methoxyl groups. Specifically, we proposed that the clumped ^{13}C–D and D/H isotopic compositions of methoxyl groups in wood are sensitive to the mixing ratio of methyl group precursors derived from photorespiration cycle intermediates vs. from Calvin cycle products, which depends on the relative rate of oxygenation vs. carboxylation by Rubisco and the fraction of photorespiratory metabolites exported to make methoxyl groups in wood. We validated this proxy by examining the isotopic composition of methoxyl groups from plants without water limitation and where either temperature or [CO_2] varied in isolation. We tested it by observing a correlation in these samples between clumped ^{13}C–D and D/H isotopic compositions, which agreed with expectations based on previous work. We then applied this proxy to a global dataset of wood formed between ~1800 and 1950 to examine how relative photorespiration rate varied with climate and water availability in an era of approximately constant atmospheric [CO_2].

We observed global trends in methoxyl clumping with daytime growing season temperature that appear to diverge with increasing temperature depending on whether an individual plant was water-limited during growth. We interpreted this to indicate that relative photorespiration rates and the fraction of photorespiratory metabolites used to make methoxyl groups vary systematically with climate such that as photorespiration rates increased due to increasing temperature, water-replete plants exported proportionally more photorespiratory metabolic intermediates to lignin. Water-limited plants responded to increasing temperature by either reducing photorespiratory export and/or redirecting more photorespiratory metabolites to systems that mitigate water loss.

These findings have the following key implications. The divergent trends of clumped isotope compositions vs. temperature in water-replete and water-limited systems indicate changes to photorespiration and thus GPP with rising [CO_2] in a warming world. Trees growing in colder climates appear to have relatively low photorespiration rates, and thus, GPP here is likely less sensitive to a further suppression of photorespiration. In warmer climates, whether a future suppression of photorespiration will increase GPP in any one environment will depend on how the global [CO_2] increase interacts with local changes in temperature and water availability, and the costs vs. benefits of exporting photorespiratory metabolites in individual plants. Finally, in addition to being a useful monitor of changes to photorespiratory metabolism in the present and future, this proxy holds promise for reconstructing relative photorespiration rates in geologic past (up to tens of millions of years ago). This would allow us to explicitly test existing hypotheses regarding the changing influence of plant photorespiration on climate (and vice versa) over geologic time.

Materials and Methods

Sample Materials. Wood samples were obtained from three sources:

1) *Pre-1950 bulk wood samples from the Forest Products Laboratory:* Most bulk wood samples were obtained from the Forest Products Laboratory at the University of California, Berkeley. A complete list of wood samples, sources, and sampling data are provided in *SI Appendix*, Tables S1 and S2. The repository houses ~1″ × 4″ × 4″ sections cut from longer boards of the main trunk of trees worldwide. Most samples (15 of 22) were from North American trees sampled as part of Project I from the New York Forest Service with the rest from same repository but chosen to provide a wider geographic range. Twenty of these wood samples were originally collected between 1934 and 1952. Among these twenty, sixteen reported tree ages, which were all less than 150 y at the time of sampling, such that most wood samples studied were formed between ~1800 and ~1950. The final two wood samples were collected in 1976 or 1977 as part of the S. Epstein (Caltech) collection, and consisted of entire trunk cross-sections including bark. For these, we specifically analyzed wood produced before 1950 by counting inwards from the last ring.

For each sample, we removed any outer bark and cambium if present. We then cut a ~5-mm-thick section against the grain with a coping saw to form a subsample for our measurement. Latewood and earlywood were mechanically separated with a razor blade where possible. In these cases, we combined latewood or earlywood from at least five annual growth rings to make one latewood sample and one earlywood sample per tree. If latewood and earlywood could not be separated, we pooled all material from at least five annual growth rings. The subsection was then powdered in a Wiley mill to produce 1–20 g of homogenized power. The saw and mill were cleaned with dry Kimwipes and compressed air between samples.

In the Main Text, we present results from latewood and whole wood (both latewood and earlywood combined) and do not distinguish between them. Comparisons between latewood and earlywood are presented and discussed in *SI Appendix*. Briefly, since earlywood is preferentially made in spring and incorporates more secondary stored carbon from previous growth years, we expect isotopic compositions to be more similar in earlywood compared to latewood in the same trees. We observed this, which supports with our central hypothesis about the controls on $\Delta^{13}CH_2D$. Whether or not earlywood isolates are included in the main dataset does not affect our conclusions.

2) *Bald cypress and giant sequoia annual and subannual tree rings:* We supplemented these whole-wood samples with tree rings from bald cypress (*Taxodium distichum*) and giant sequoia (*Sequoiadendron giganteum*) cores.

The bald cypress sample comes from Arbuckle Creek, in south-central Florida, which retains a remnant stand of uncut old growth bald cypress trees present on the low-lying floodplain downstream from Lake Arbuckle. Some of the living bald cypress trees are large (1.5 to 3 m diameter at breast height) and over 300 y old. The derived tree-ring chronology extends from 1232 to 2018 and is based on both living trees and remnant wood found preserved on the floodplain. The specific core sample used in this study (ABC10B) was obtained from a living bald cypress at least 210 years old located at 27.65353N, 81.372456W, and at 19.4 m above sea level. The 5-mm-diameter core was extracted with a Swedish increment borer just above the basal swell on June 11, 2019, and each annual ring on ABC10B was dated to the exact calendar year of formation with dendrochronology.

Three giant sequoia (*Sequoiadendron giganteum*) specimens were studied that grew along the bank of Strawberry Creek, UC Berkeley campus, Berkeley, CA, USA (UCB-SEGI-1 and -2) or the Freeman Creek Grove, Southern Sierra Nevada,

CA USA (TD-FCUG-A-1). Specific sample locations are reported in *SI Appendix*, Table S1. All specimens were sampled using a 12-mm-diameter incremental borer at breast height following methods in ref. 101. Ages were determined by dendrochronology.

For all tree cores, rings from targeted time intervals were sectioned manually using a razor blade and powdered using a tungsten-carbide ball mill (Spex Sampleprep 8000). The ball mill was cleaned with compressed air, dry Kimwipes, and precombusted silica sand between samples. For the bald cypress core, we analyzed five samples, each consisting of a consecutive 10-y interval (for the first four) or 15-y interval (for the period of 2005 to 2019 due to decreasing ring width) that in total span the last 200 y (*SI Appendix*, Table S7). For each of the three giant sequoia cores, we created one sample of earlywood and one of latewood combining multiple years of growth, all from before 1950.

3) *Basal shoots from high [CO_2] Ginkgo biloba trees from Ginkgo growth experiment:* Basal root shoots from the 2020 growing season of the Fossil Atmospheres experiment (62) were excised from living trees in November 2020 and dried at 40 °C for 3 d. Bark and cambium were removed with razor blades and not analyzed. Xylem wood was powdered using a tungsten-carbide ball mill and cleaned between samples as described above.

Methoxyl Derivatization and Analysis. Wood methoxyl groups were derivatized, purified, and analyzed using established methods described in ref. 35. Briefly, wood powders were reacted for 2 h with preboiled, 57% hydriodic acid (99.5% purity, stabilized, Sigma Aldrich) at reflux (130 °C). Evolved iodomethane (CH_3I) was entrained in helium and continuously frozen in liquid N_2 for the duration of the reaction. CH_3I was purified using cryogenic and chemical steps on a glass vacuum line and quantitatively converted to chloromethane (CH_3Cl) by reaction with a >10× molar excess of silver chloride (99.5% purity, Sigma Aldrich) at 80 °C for 14–40 h. Resulting CH_3Cl was purified with additional cryogenic steps and stored in a Pyrex break-seal until analysis. Isotopic compositions of CH_3Cl were measured by dual-inlet high-resolution isotope-ratio mass spectrometry (IRMS) on a Thermo Scientific 253 Ultra at UC Berkeley and reported relative to VPDB (for $\delta^{13}C$), VSMOW (for δD), or the stochastic reference frame (for $\Delta^{13}CH_2D$ and $\Delta^{12}CHD_2$) following ref. 35. $\Delta^{12}CHD_2$ is defined as $\Delta^{12}CHD_2 = ({}^{12CHD2}R/{}^{12CHD2}R^{*}-1)\times 1000$, where ${}^{12CHD2}R = [{}^{12}CHD_2]/[{}^{12}CH_3]$ and * indicates the stochastic abundance. Individual measurements are reported in *SI Appendix*, Table S3, and sample averages are reported in *SI Appendix*, Table S4. Typical 1σ external reproducibility (i.e., full procedural replicates) of wood methoxyl isotopic compositions is 0.5‰ for $\delta^{13}C$, 1‰ for δD, 0.25‰ for $\Delta^{13}CH_2D$, and 2.5‰ for $\Delta^{12}CHD_2$.

Climate Variables and Mean Growing Season Temperature. Elevation and mean monthly temperature, precipitation, and cloud cover were estimated for each wood sample using the nearest 10-minute grid point from the CRU CL v.2.0 dataset of mean monthly climate for the period of 1961–1990 (102). Mean monthly soil moisture and evapotranspiration fluxes were computed from these inputs using SPLASH v.1.0 (103). Following ref. 104, the growing season for each site was defined as the set of consecutive months with an average temperature above 5 °C and precipitation/equilibrium evapotranspiration > 0.05. Daytime temperatures were estimated as the average of the daily mean temperature and daily maximum temperature for each day in an average year as computed in SPLASH (103). Mean daytime growing season temperatures were the average of daily daytime temperatures for all months in the growing season. The annual isotopic composition of source water for each tree was estimated using the Online Isotopes In Precipitation Calculator (OIPC) v.3.1 (65, 66, 105), following previous work (31, 34, 58).

Determination and Categorization of Water Availability during Growth. Where possible, we categorized samples as having grown in water-limited or water-replete environments. We made these categorizations based on original collection notes for samples and/or historical climate data. A sample was determined to be water-replete only if it met either of the following conditions: 1) sample collection notes indicated tree was growing in a perennial standing water body, immediately next to a perennial standing water body, or had a root system that penetrated the water table; or 2) the historical climate data from CRU CL v.2.0, when used as an input to SPLASH v.1.0, found that soil moisture was at or above capacity (continuous runoff) throughout the growing season. *Ginkgo* growth experiments were watered regularly and thus also assigned to be water-replete.

Model Estimates of Oxygenation and Carboxylation Rates. Relative photorespiration rates of RuBP oxygenation (V_O) to carboxylation (V_C) by Rubisco were estimated using the steady-state mechanistic leaf photosynthesis model of Farquhar, von Caemmerer & Berry (FvCB; 8) and the temperature response functions of ref. 10. In doing the modeling, we assumed that the ratio of c_i/atmospheric [CO_2] is 0.7 at 25 °C and depends on temperature following ref. 106: i.e., from 20 to 30 °C, c_i/atmospheric [CO_2] decreases from 0.8 to 0.6. We assumed an atmospheric [CO_2] value of 300 ppm for all samples grown between ~1,800 and 1,950, except for the bald cypress tree where the specific average [CO_2] during each growth interval was used (*SI Appendix*, Table S7). Incorporating the effect of mesophyll conductance, which has been shown to scale with stomatal conductance by a factor that is approximately constant worldwide (107), increases the sensitivity of V_O/V_C to atmospheric [CO_2] by lowering [CO_2] in the chloroplasts by an approximately constant factor but does not change our interpretations (*SI Appendix*). We assumed a constant atmospheric [O_2] of 21%. In *SI Appendix*, we explore the effect of relaxing some of these assumptions by implementing a more complex model that incorporates the effects of water stress and the acclimation of photosynthetic parameters to local climate throughout the growing season [*P*-model v.1.0, (63, 64)]. The *P*-model compresses the range of V_O/V_C values predicted in samples from different climates by up to 30% relative but does not impact the significance of the correlation between $\Delta^{13}CH_2D$ and V_O/V_C. Because we do not interpret V_O/V_C values quantitatively, choice of model does not affect our interpretations (see *SI Appendix* for details).

Data, Materials, and Software Availability. All study data are included in the article and/or *SI Appendix*. All study data and software code used to generate all figures and analyses have been deposited and are freely available on ScholarSphere [DOI: 10.26207/zcnm-0x09 and 10.26207/6a4k-sf79].

ACKNOWLEDGMENTS. We are indebted to J. Shelley and the Forest Products Laboratory at UC Berkeley for providing archived samples and laboratory facilities. X. Feng and J. Landis (Dartmouth University) also graciously provided samples. K. Freeman (Penn State) provided additional laboratory facilities. J. Berry and J. Johnson (Carnegie Institution for Science) and L. Anderegg (UC Berkeley) provided helpful suggestions at early stages of this project. Editor Donald Ort and three anonymous reviewers provided thoughtful comments that greatly improved the clarity and scope of the paper. M.K.L. and R.A.S. each acknowledge the support from Agouron Institute Geobiology Postdoctoral Fellowships. DAS acknowledges the support from the NSF under Grant No. EAR-2047003. The Thermo 253 Ultra was funded in part by the Heising-Simons Foundation.

Author affiliations: [a]Department of Earth and Planetary Science, University of California, Berkeley, CA 94720; [b]Department of Geosciences, The Pennsylvania State University, University Park, PA 16802; [c]Department of Chemistry and Physical Sciences, Quinnipiac University, Hamden, CT 06518; [d]Department of Earth, Environmental, and Planetary Sciences, Brown University, Providence, RI 02912; [e]Department of Paleobiology, National Museum of Natural History, Smithsonian Institution, Washington, DC 20560; [f]Department of Geosciences, University of Arkansas, Fayetteville, AR 72701; and [g]Department of Integrative Biology, University of California, Berkeley, CA 94720

1. R. A. Berner, *The Phanerozoic Carbon Cycle: CO_2 and O_2* (Oxford University Press on Demand, 2004).
2. P. Ciais *et al.*, "Carbon and other biogeochemical cycles" in *Climate Change 2013: The Physical Science Basis in Contribution of Working Group I to the Fifth Assessment Report of the Intergovernmental Panel on Climate Change* (Cambridge University Press, 2014), pp. 465–570.
3. Intergovernmental Panel on Climate Change (IPCC), Ed., "Global carbon and other biogeochemical cycles and feedbacks" in *Climate Change 2021–The Physical Science Basis: Working Group I Contribution to the Sixth Assessment Report of the Intergovernmental Panel on Climate Change* (Cambridge University Press, 2023), pp. 673–816.
4. R. A. Berner, Weathering, plants, and the long-term carbon cycle. *Geochim. Cosmochim. Acta* **56**, 3225–3231 (1992).
5. M. P. D'Antonio, D. E. Ibarra, C. K. Boyce, Land plant evolution decreased, rather than increased, weathering rates. *Geology* **48**, 29–33 (2019).
6. J. Shukla, Y. Mintz, Influence of land-surface evapotranspiration on the Earth's climate. *Science* **215**, 1498–1501 (1982).
7. C. K. Boyce, J.-E. Lee, Plant evolution and climate over geological timescales. *Annu. Rev. Earth Planet. Sci.* **45**, 61–87 (2017).

8. G. D. Farquhar, S. von Caemmerer, J. A. Berry, A biochemical model of photosynthetic CO_2 assimilation in leaves of C_3 species. *Planta* **149**, 78–90 (1980).
9. J. T. Ball, I. E. Woodrow, J. A. Berry, "A model predicting stomatal conductance and its contribution to the control of photosynthesis under different environmental conditions" in *Progress in Photosynthesis Research: Volume 4 Proceedings of the VIIth International Congress on Photosynthesis Providence, RI, August 10–15, 1986*, J. Biggins, Ed. (Springer, Netherlands, 1987), pp. 221–224.
10. C. J. Bernacchi, E. L. Singsaas, C. Pimentel, A. R. P. Jr., S. P. Long, Improved temperature response functions for models of Rubisco-limited photosynthesis. *Plant Cell Environ.* **24**, 253–259 (2001).
11. W. Kolby Smith *et al.*, Large divergence of satellite and Earth system model estimates of global terrestrial CO_2 fertilization. *Nat. Climate Change* **6**, 306–310 (2015).
12. M. Jiang *et al.*, The fate of carbon in a mature forest under carbon dioxide enrichment. *Nature* **580**, 227–231 (2020).
13. P. Friedlingstein *et al.*, Uncertainties in CMIP5 climate projections due to carbon cycle feedbacks. *J. Climate* **27**, 511–526 (2014).
14. V. K. Arora *et al.*, Carbon–concentration and carbon–climate feedbacks in CMIP6 models and their comparison to CMIP5 models. *Biogeosciences* **17**, 4173–4222 (2020).
15. G. Wohlfahrt, L. Gu, The many meanings of gross photosynthesis and their implication for photosynthesis research from leaf to globe. *Plant Cell Environ.* **38**, 2500–2507 (2015).
16. D. T. Canvin, "Photorespiration: Comparison between C_3 and C_4 plants" in *Photosynthesis II: Photosynthetic Carbon Metabolism and Related Processes, Encyclopedia of Plant Physiology*, M. Gibbs, E. Latzko, Eds. (Springer, 1979), pp. 368–396.
17. A. Wingler, P. J. Lea, W. P. Quick, R. C. Leegood, Photorespiration: Metabolic pathways and their role in stress protection. *Phil. Trans. R. Soc. Lond. B* **355**, 1517–1529 (2000).
18. H. Bauwe, M. Hagemann, A. R. Fernie, Photorespiration: Players, partners and origin. *Trends Plant Sci.* **15**, 330–336 (2010).
19. R. F. Sage, T. L. Sage, F. Kocacinar, Photorespiration and the evolution of C_4 photosynthesis. *Annu. Rev. Plant Biol.* **63**, 19–47 (2012).
20. T. D. Sharkey, Estimating the rate of photorespiration in leaves. *Physiol. Plant.* **73**, 147–152 (1988).
21. A. Brooks, G. D. Farquhar, Effect of temperature on the CO_2/O_2 specificity of ribulose-1,5-bisphosphate carboxylase/oxygenase and the rate of respiration in the light. *Planta* **165**, 397–406 (1985).
22. R. F. Sage, D. S. Kubien, The temperature response of C_3 and C_4 photosynthesis. *Plant Cell Environ.* **30**, 1086–1106 (2007).
23. F. A. Busch, Current methods for estimating the rate of photorespiration in leaves. *Plant Biol.* **15**, 648–655 (2013).
24. I. Ehlers *et al.*, Detecting long-term metabolic shifts using isotopomers: CO_2-driven suppression of photorespiration in C_3 plants over the 20th century. *Proc. Natl. Acad. Sci. U.S.A.* **112**, 15585–15590 (2015).
25. E. B. Wilkes *et al.*, Position-specific carbon isotope analysis of serine by gas chromatography/Orbitrap mass spectrometry, and an application to plant metabolism. *Rapid Commun. Mass Spectrom.* **36**, e9347 (2022).
26. H. Serk *et al.*, Global CO_2 fertilization of Sphagnum peat mosses via suppression of photorespiration during the twentieth century. *Sci. Rep.* **11**, 24517 (2021).
27. A. D. Hanson, S. Roje, One-carbon metabolism in higher plants. *Ann. Rev. Plant Physiol. Plant Mol. Biol.* **52**, 119–137 (2001).
28. F. Keppler, R. M. Kalin, D. B. Harper, W. C. Mcroberts, J. T. G. Hamilton, Carbon isotope anomaly in the major plant C_1 pool and its global biogeochemical implications. *Biogeosciences* **1**, 123–131 (2004).
29. M. K. Lloyd *et al.*, Methoxyl stable isotopic constraints on the origins and limits of coal-bed methane. *Science* **374**, 894–897 (2021).
30. T. J. Porter *et al.*, Canadian arctic neogene temperatures reconstructed from hydrogen isotopes of lignin–methoxy groups from sub-fossil wood. *Paleoceanogr. Paleoclimatol.* **37**, e2021PA004345 (2022).
31. F. Keppler *et al.*, Stable hydrogen isotope ratios of lignin methoxyl groups as a paleoclimate proxy and constraint of the geographical origin of wood. *New Phytol.* **176**, 600–609 (2007).
32. Y. Gori *et al.*, Carbon, hydrogen and oxygen stable isotope ratios of whole wood, cellulose and lignin methoxyl groups of *Picea abiesas* climate proxies. *Rapid Commun. Mass Spectrom.* **27**, 265–275 (2012).
33. S. J. Feakins, P. V. Ellsworth, L. da Silveira Lobo Sternberg, Lignin methoxyl hydrogen isotope ratios in a coastal ecosystem. *Geochim. Cosmochim. Acta* **121**, 54–66 (2013).
34. M. Greule, A. Wieland, F. Keppler, Measurements and applications of δ^2H values of wood lignin methoxy groups for paleoclimatic studies. *Q Sci. Rev.* **268**, 107107 (2021).
35. M. K. Lloyd, D. L. Eldridge, D. A. Stolper, Clumped $^{13}CH_2D$ and $^{12}CHD_2$ compositions of methyl groups from wood and synthetic monomers: Methods, experimental and theoretical calibrations, and initial results. *Geochim. Cosmochim. Acta* **297**, 233–275 (2021).
36. R. Ros, J. Muñoz-Bertomeu, S. Krueger, Serine in plants: Biosynthesis, metabolism, and functions. *Trends Plant Sci.* **19**, 564–569 (2014).
37. V. Prabhu, K. B. Chatson, G. D. Abrams, J. King, ^{13}C nuclear magnetic resonance detection of interactions of serine hydroxymethyltransferase with C1-tetrahydrofolate synthase and glycine decarboxylase complex activities in *Arabidopsis*. *Plant Physiol.* **112**, 207–216 (1996).
38. H. Ziegler, "Nature of transported substances" in *Transport in Plants I: Phloem Transport in Encyclopedia of Plant Physiology*, M. H. Zimmermann, J. A. Milburn, Eds. (Springer, 1975), pp. 59–100.
39. A. Augusti, T. R. Betson, J. Schleucher, Hydrogen exchange during cellulose synthesis distinguishes climatic and biochemical isotope fractionations in tree rings. *New Phytol.* **172**, 490–499 (2006).
40. M.-A. Cormier *et al.*, ^{2}H-fractionations during the biosynthesis of carbohydrates and lipids imprint a metabolic signal on the δ^2H values of plant organic compounds. *New Phytol.* **218**, 479–491 (2018).
41. J. Schleucher, "Intramolecular deuterium distributions and plant growth conditions" in *Stable Isotopes: Integration of Biological, Ecological and Geochemical Processes* (BIOS Scientific Publishers, Oxford, UK, 1998), pp. 63–73.
42. T. Wieloch *et al.*, Metabolism is a major driver of hydrogen isotope fractionation recorded in tree-ring glucose of *Pinus nigra*. *New Phytol.* **234**, 449–461 (2022).
43. G. Tcherkez, A. Mahé, M. Hodges, $^{12}C/^{13}C$ fractionations in plant primary metabolism. *Trends Plant Sci.* **16**, 499–506 (2011).
44. G. Tcherkez, G. D. Farquhar, Viewpoint: Carbon isotope effect predictions for enzymes involved in the primary carbon metabolism of plant leaves. *Funct. Plant Biol.* **32**, 277 (2005).
45. P. C. Harley, T. D. Sharkey, An improved model of C_3 photosynthesis at high CO_2: Reversed O_2 sensitivity explained by lack of glycerate reentry into the chloroplast. *Photosynth. Res.* **27**, 169–178 (1991).
46. C. Abadie, E. R. A. Boex-Fontvieille, A. J. Carroll, G. Tcherkez, In vivo stoichiometry of photorespiratory metabolism. *Nat. Plants* **2**, 1–4 (2016).
47. F. A. Busch, R. F. Sage, G. D. Farquhar, Plants increase CO_2 uptake by assimilating nitrogen via the photorespiratory pathway. *Nat. Plants* **4**, 46–54 (2018).
48. X. Fu, L. M. Gregory, S. E. Weise, B. J. Walker, Integrated flux and pool size analysis in plant central metabolism reveals unique roles of glycine and serine during photorespiration. *Nat. Plants* **9**, 169–178 (2023).
49. T. D. Sharkey, O_2-insensitive photosynthesis in C_3 plants: Its occurrence and a possible explanation. *Plant Physiol.* **78**, 71–75 (1985).
50. B. Riens, G. Lohaus, D. Heineke, H. W. Heldt, Amino acid and sucrose content determined in the cytosolic, chloroplastic, and vacuolar compartments and in the phloem sap of spinach leaves. *Plant Physiol.* **97**, 227–233 (1991).
51. R. Ros *et al.*, Serine biosynthesis by photorespiratory and non-photorespiratory pathways: an interesting interplay with unknown regulatory networks. *Plant Biol.* **15**, 707–712 (2013).
52. F. A. Busch, Photorespiration in the context of Rubisco biochemistry, CO_2 diffusion and metabolism. *Plant J.* **101**, 919–939 (2020).
53. C. Abadie, S. Blanchet, A. Carroll, G. Tcherkez, Metabolomics analysis of postphotosynthetic effects of gaseous O_2 on primary metabolism in illuminated leaves. *Funct. Plant Biol.* **44**, 929–940 (2017).
54. C. Abadie, C. Bathellier, G. Tcherkez, Carbon allocation to major metabolites in illuminated leaves is not just proportional to photosynthesis when gaseous conditions (CO_2 and O_2) vary. *New Phytol.* **218**, 94–106 (2018).
55. J. M. Eiler, "Clumped-isotope" geochemistry–The study of naturally-occurring, multiply-substituted isotopologues. *Earth Planet. Sci. Lett.* **262**, 309–327 (2007).
56. Z. Wang, E. A. Schauble, J. M. Eiler, Equilibrium thermodynamics of multiply substituted isotopologues of molecular gases. *Geochim. Cosmochim. Acta* **68**, 4779–4797 (2004).
57. L. Y. Yeung, Combinatorial effects on clumped isotopes and their significance in biogeochemistry. *Geochim. Cosmochim. Acta* **172**, 22–38 (2016).
58. T. Anhäuser, M. Greule, D. Polag, G. J. Bowen, F. Keppler, Mean annual temperatures of mid-latitude regions derived from δ^2H values of wood lignin methoxyl groups and its implications for paleoclimate studies. *Sci. Total Environ.* **574**, 1276–1282 (2017).
59. H. L. Schmidt, R. A. Werner, W. Eisenreich, Systematics of ^{2}H patterns in natural compounds and its importance for the elucidation of biosynthetic pathways. *Phytochem. Rev.* **2**, 61–85 (2003).
60. B. E. Medlyn *et al.*, Reconciling the optimal and empirical approaches to modelling stomatal conductance: Reconciling optimal and empirical stomatal models. *Global Change Biol.* **17**, 2134–2144 (2011).
61. M. L. Bender, T. Sowers, J.-M. Barnola, J. Chappellaz, Changes in the O_2/N_2 ratio of the atmosphere during recent decades reflected in the composition of air in the firn at Vostok Station, Antartica. *Geophys. Res. Lett.* **21**, 189–192 (1994).
62. M. A. Scher *et al.*, The effect of CO_2 concentration on carbon isotope discrimination during photosynthesis in *Ginkgo biloba*: implications for reconstructing atmospheric CO_2 levels in the geologic past. *Geochim. Cosmochim. Acta* **337**, 82–94 (2022).
63. H. Wang *et al.*, Towards a universal model for carbon dioxide uptake by plants. *Nat. Plants* **3**, 734–741 (2017).
64. B. D. Stocker *et al.*, P-model v1.0: An optimality-based light use efficiency model for simulating ecosystem gross primary production. *Geosci. Model Dev.* **13**, 1545–1581 (2020).
65. G. J. Bowen, J. Revenaugh, Interpolating the isotopic composition of modern meteoric precipitation. *Water Resources Res.* **39**, 1299 (2003).
66. G. J. Bowen, The Online Isotopes in Precipitation Calculator, version 3.1. (2021). https://www.waterisotopes.org. Accessed 15 June 2022.
67. C. D. Keeling *et al.*, "Atmospheric CO_2 and $^{13}CO_2$ Exchange with the terrestrial biosphere and oceans from 1978 to 2000: Observations and carbon cycle implications" in *A History of Atmospheric CO_2 and Its Effects on Plants, Animals, and Ecosystems, Ecological Studies*, I. T. Baldwin *et al.*, Eds. (Springer, 2005), pp. 83–113.
68. B. R. Helliker, S. L. Richter, Subtropical to boreal convergence of tree–leaf temperatures. *Nature* **454**, 511–514 (2008).
69. B. R. Helliker *et al.*, Assessing the interplay between canopy energy balance and photosynthesis with cellulose δ^{18}O: Large-scale patterns and independent ground-truthing. *Oecologia* **187**, 995–1007 (2018).
70. J. Berry, O. Bjorkman, Photosynthetic response and adaptation to temperature in higher plants. *Annu. Rev. Plant. Physiol.* **31**, 491–543 (1980).
71. K. Raschke, A. Resemann, The midday depression of CO_2 assimilation in leaves of *Arbutus unedo* L.: Diurnal changes in photosynthetic capacity related to changes in temperature and humidity. *Planta* **168**, 546–558 (1986).
72. G. Zotz, K. Winter, "Diel patterns of CO_2 exchange in rainforest canopy plants" in *Tropical Forest Plant Ecophysiology*, S. S. Mulkey, R. L. Chazdon, A. P. Smith, Eds. (Springer US, 1996), pp. 89–113.
73. L. A. Cernusak *et al.*, Tropical forest responses to increasing atmospheric CO_2: Current knowledge and opportunities for future research. *Funct. Plant Biol.* **40**, 531–551 (2013).
74. M. Hanin *et al.*, Plant dehydrins and stress tolerance. *Plant Signaling Behav.* **6**, 1503–1509 (2014).
75. R. C. Dirks, M. Singh, G. S. Potter, L. G. Sobotka, J. Schaefer, Carbon partitioning in soybean (*Glycine max*) leaves by combined ^{11}C and ^{13}C labeling. *New Phytol.* **196**, 1109–1121 (2012).
76. F. A. Busch, T. L. Sage, A. B. Cousins, R. F. Sage, C_3 plants enhance rates of photosynthesis by reassimilating photorespired and respired CO_2. *Plant Cell Environ.* **36**, 200–212 (2013).
77. B. J. Walker, A. VanLoocke, C. J. Bernacchi, D. R. Ort, The costs of photorespiration to food production now and in the future. *Annu. Rev. Plant Biol.* **67**, 107–129 (2016).
78. D. Schimel, B. B. Stephens, J. B. Fisher, Effect of increasing CO_2 on the terrestrial carbon cycle. *Proc. Natl. Acad. Sci. U.S.A.* **112**, 436–441 (2015).
79. W. Cramer *et al.*, Global response of terrestrial ecosystem structure and function to CO_2 and climate change: Results from six dynamic global vegetation models. *Global Change Biol.* **7**, 357–373 (2001).
80. J. E. Campbell *et al.*, Large historical growth in global terrestrial gross primary production. *Nature* **544**, 84–87 (2017).
81. A. P. Walker *et al.*, Integrating the evidence for a terrestrial carbon sink caused by increasing atmospheric CO_2. *New Phytol.* **229**, 2413–2445 (2021).
82. A. Kozaki, G. Takeba, Photorespiration protects C_3 plants from photooxidation. *Nature* **384**, 557–560 (1996).
83. S. Takahashi, M. R. Badger, Photoprotection in plants: A new light on photosystem II damage. *Trends Plant Sci.* **16**, 53–60 (2011).

84. A. J. Bloom, Photorespiration and nitrate assimilation: A major intersection between plant carbon and nitrogen. *Photosynth. Res.* **123**, 117–128 (2015).
85. L. V. Kurepin *et al.*, Contrasting acclimation abilities of two dominant boreal conifers to elevated CO_2 and temperature. *Plant, Cell Environ.* **41**, 1331–1345 (2018).
86. M. E. Dusenge, S. Madhavji, D. A. Way, Contrasting acclimation responses to elevated CO_2 and warming between an evergreen and a deciduous boreal conifer. *Global Change Biol.* **26**, 3639–3657 (2020).
87. B. D. Sigurdsson, J. L. Medhurst, G. Wallin, O. Eggertsson, S. Linder, Growth of mature boreal Norway spruce was not affected by elevated [CO_2] and/or air temperature unless nutrient availability was improved. *Tree Physiol.* **33**, 1192–1205 (2013).
88. M. E. Dusenge, A. G. Duarte, D. A. Way, Plant carbon metabolism and climate change: Elevated CO_2 and temperature impacts on photosynthesis, photorespiration and respiration. *New Phytol.* **221**, 32–49 (2019).
89. J. Peñuelas, J. G. Canadell, R. Ogaya, Increased water-use efficiency during the 20th century did not translate into enhanced tree growth. *Global Ecol. Biogeogr.* **20**, 597–608 (2011).
90. J. Lloyd, G. D. Farquhar, Effects of rising temperatures and [CO_2] on the physiology of tropical forest trees. *Philos. Trans. R. Soc. B Biol. Sci.* **363**, 1811–1817 (2008).
91. D. B. Clark, D. A. Clark, S. F. Oberbauer, Annual wood production in a tropical rain forest in NE Costa Rica linked to climatic variation but not to increasing CO_2. *Global Change Biol.* **16**, 747–759 (2010).
92. M. Eisenhut *et al.*, Photorespiration is crucial for dynamic response of photosynthetic metabolism and stomatal movement to altered CO_2 availability. *Mol. Plant* **10**, 47–61 (2017).
93. C. Grossiord *et al.*, Plant responses to rising vapor pressure deficit. *New Phytol.* **226**, 1550–1566 (2020).
94. W. Jiao *et al.*, Observed increasing water constraint on vegetation growth over the last three decades. *Nat. Commun.* **12**, 3777 (2021).
95. P. G. Hatcher, D. J. Clifford, The organic geochemistry of coal: From plant materials to coal. *Org. Geochem.* **27**, 251–274 (1997).
96. A. Drobniak, M. Mastalerz, Chemical evolution of Miocene wood: Example from the Belchatow brown coal deposit, central Poland. *Int. J. Coal Geol.* **66**, 157–178 (2006).
97. T. Anhäuser, B. A. Hook, J. Halfar, M. Greule, F. Keppler, Earliest Eocene cold period and polar amplification–Insights from δ^2H values of lignin methoxyl groups of mummified wood. *Palaeogeogr., Palaeoclimatol., Palaeoecol.* **505**, 326–336 (2018).
98. J. K. Ward *et al.*, Carbon starvation in glacial trees recovered from the La Brea tar pits, southern California. *Proc. Natl. Acad. Sci. U.S.A.* **102**, 690–694 (2005).
99. L. M. Gerhart, J. K. Ward, Plant responses to low [CO_2] of the past. *New Phytol.* **188**, 674–695 (2010).
100. M. Pagani, K. Caldeira, R. Berner, D. J. Beerling, The role of terrestrial plants in limiting atmospheric CO_2 decline over the past 24 million years. *Nature* **460**, 85–88 (2009).
101. J. S. Roden, J. A. Johnstone, T. E. Dawson, Intra-annual variation in the stable oxygen and carbon isotope ratios of cellulose in tree rings of coast redwood (*Sequoia sempervirens*). *Holocene* **19**, 189–197 (2009).
102. M. New, D. Lister, M. Hulme, I. Makin, A high-resolution data set of surface climate over global land areas. *Climate Res.* **21**, 1–25 (2002).
103. T. W. Davis *et al.*, Simple process-led algorithms for simulating habitats (SPLASH vol 1.0): Robust indices of radiation, evapotranspiration and plant-available moisture. *Geosci. Model Dev.* **10**, 689–708 (2017).
104. I. J. Wright *et al.*, Global climatic drivers of leaf size. *Science* **357**, 917–921 (2017).
105. IAEA/WMO, Global Network of Isotopes in Precipitation. GNIP Database. https://www.iaea.org/water. Accessed 20 June 2020.
106. S. P. Long, Modification of the response of photosynthetic productivity to rising temperature by atmospheric CO_2 concentrations: Has its importance been underestimated? *Plant Cell Environ.* **14**, 729–739 (1991).
107. X. Y. Gong *et al.*, Overestimated gains in water-use efficiency by global forests. *Global Change Biol.* **28**, 4923–4934 (2022).